Scientific Research Publishing

Journal of Computer and Communications, 2022, 10, 72-90
https://www.scirp.org/journal/jcc
ISSN Online: 2327-5227
ISSN Print: 2327-5219

Security in Multicast Over α-μ Fading Channels with Orthogonal Frequency Division Multiplexing

Mohammad Mahmud Hasan, Md. Zahurul Islam Sarkar

Department of Electrical and Electronic Engineering, Rajshahi University of Engineering and Technology, Rajshahi, Bangladesh
Email: mmh_mahmudhasan@yahoo.com, msarkar01@qub.ac.uk

How to cite this paper: Hasan, M.M. and Sarkar, M.Z.I. (2022) Security in Multicast Over α-μ Fading Channels with Orthogonal Frequency Division Multiplexing. *Journal of Computer and Communications*, **10**, 72-90.
https://doi.org/10.4236/jcc.2022.1011006

Received: September 27, 2022
Accepted: November 14, 2022
Published: November 17, 2022

Abstract

The orthogonal space-frequency block coding (OSFBC) with orthogonal frequency division multiplexing (OFDM) system reduces complexity in the receiver which improves the system performance significantly. Motivated by these advantages of OSFBC-OFDM system, this paper considers a secure wireless multicasting scenario through multiple-input multiple-output (MIMO) OFDM system employing OSFBC over frequency selective α-μ fading channels. The authors are interested to protect the desired signals from eavesdropping considering the impact of the number of multicast users and eavesdroppers, and the fading parameters α and μ. A mathematical model has been developed based on the closed-form analytical expressions of the probability of non-zero secrecy multicast capacity (PNSMC) and the secure outage probability for multicasting (SOPM) to ensure the security in the presence of multiple eavesdroppers. The results show that the security in MIMO OSFBC OFDM system over α-μ fading is more sensitive to the magnitude of α and μ and this effect increases in the high signal-to-noise ratio (SNR) region of the main channel.

Keywords

Orthogonal Space-Frequency Block Coding, Orthogonal Frequency Division Multiplexing, Probability of Non-Zero Secrecy Multicast Capacity, Secure Outage Probability for Multicasting

1. Introduction

The orthogonal space-frequency block coding (OSFBC) with orthogonal frequency division multiplexing (OFDM) system reduces complexity in the receiver

which improves the system performance significantly [1]. On the other hand, multicasting is an efficient wireless communication technique for group-oriented and personal communication such as video-conferencing, e-learning, etc. Due to the increase of application areas and the mobility of users with network components, the security is a crucial aspect in wireless multicasting systems because of the fact that the medium of wireless multicasting is susceptible to eavesdropping and fraud [2].

1.1. Related Works

In this paper, authors concentrate on the security in multicasting employing the OSFBC technique with MIMO-OFDM system over frequency selective α-μ fading channels. Although a good number of publications are available in the literature to describe the security in α-μ fading channels, but there is no work which is closely related to the MIMO-OFDM system employing the OSFBC technique. Just to clarify the status of the existing literature, authors presented some recent papers which describe the status of proposed research domain. The research gap is also mentioned at the end of the related work section.

Recently, Mathur *et al.* [3] investigated the effect of correlation on the security in α-μ fading channel through asymptotic analysis. The effects of various system parameters on the secrecy diversity gain were investigated in [4]. The effects of various system parameters on the secrecy diversity and array gain were investigated in [5]. In [6], Hanif *et al.* investigated the effects of α-μ fading parameters on the security performance of multicasting scenario. In [7], the authors investigated the effects of α-μ fading parameters on the secrecy diversity parameters. The MIMO-OFDM system was considered in [8] to investigate the secrecy performance. In [9], the effects of α-μ fading parameters on the security in underlay cognitive radio network were investigated considering a single-input multiple-output (SIMO) network. In [10], authors analyzed the reliability and security of cascaded α-μ fading channels deriving the closed-form analytical expressions for the probability of non-zero secrecy capacity, the secure outage probability and the average secrecy capacity in terms of Foxs H-function. The asymptotic closed-form expression for the secrecy outage probability of SIMO α-μ fading channel were derived in [11] in terms of Foxs H-function.

However, in the aforementioned works, the authors did not consider the OSFBC system in the α-μ fading channel. Employing OSFBC in MIMO-OFDM system, the system performance can be significantly improved which is shown in [1]. Motivated by advantages of OSFBC in MIMO-OFDM system and the importance of security in multicasting, the authors of this paper investigated a secure wireless multicasting scenario in the α-μ fading channel employing OSFBC in MIMO-OFDM system.

1.2. Contributions

Based on the aforementioned scenario available in the literature and motivated by the importance of security in α-μ fading channel employing OSFBC in MIMO-

OFDM system, in this paper, authors studied a secure wireless multicasting scenario and developed a mathematical model to ensure the security in α-μ fading channel incorporating the benefits of OSFBC in MIMO-OFDM system. The major contributions of this paper can be summarized as follows.

- At first, based on the PDF of MIMO OSFBC OFDM system over α-μ fading channels, authors derived the expressions for the probability density function (PDFs) of minimum SNR of the multicast channels denoted by $d_{\min}$ and the maximum SNR of eavesdropper's channels denoted by $d_{\max}$.
- Secondly, using the PDFs of $d_{\min}$ and $d_{\max}$, authors derived the expressions for the probability of non-zero secrecy multicast capacity (PNSMC) and the secure outage probability for multicasting (SOPM).
- Finally, the effects of fading parameters α and μ, and the number of multicast users and eavesdroppers are investigated on the security in wireless multicasting through α-μ fading channels.

All the results of analysis are carried out by Mathematica and the figures are plotted by Excel.

The remainder of this paper is organized as follows. Sections II and III describe the system model and problem formulation, respectively. The expressions for the probability of non zero secrecy multicast capacity and the secure outage probability for multicasting are derived respectively in Section IV and V. Numerical results are presented in Section VI. Finally, Section VII draws the conclusions of this work.

2. System Model

A secure wireless multicasting scenario as shown in **Figure 1** is considered through MIMO OSFBC OFDM system over α-μ fading channel in the presence of N eavesdroppers. A transmitter equipped with n_t antennas sends a common stream of confidential information to the M receivers each with n_r antennas. N eavesdroppers each with n_e antennas try to decode this confidential information. Authors are interested to protect this information from eavesdropping. The channel between transmitter and receiver is known as main channel and the channel between transmitter and eavesdropper is known as eavesdropper's channel. We consider α-μ fading channels for both main channel and eavesdropper's channel. Both α and μ are the arbitrary fading parameters. α reflects the nonlinearity and μ reflects the clustering. α_m and μ_m are assumed to be the arbitrary fading parameters of the main channel while α_e and μ_e are assumed to be the arbitrary fading parameters of the eavesdropper's channel.

3. Problem Formulation

3.1. PDF of Multicast Channel

Let γ_{M_i} denotes the signal-to-noise ratio (SNR) of ith multicast channel. Then, the PDF of γ_{M_i} for MIMO OSFBC OFDM system over α-μ fading channel is given by [1].

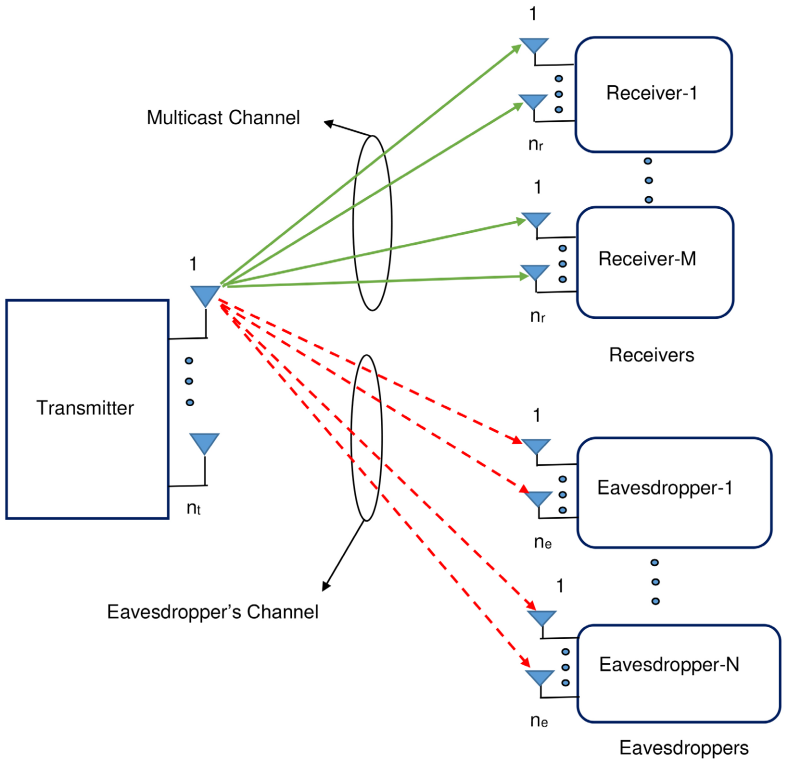

Figure 1. System model.

$$f_{\gamma_{M_i}}\left(\gamma_{M_i}\right)=\frac{\alpha_1}{2\gamma_{M_i}\Gamma\left(\mu_1\right)}\left\{\frac{\gamma_{M_i}\Gamma\left(\frac{2}{\alpha_1}+\mu_1\right)}{\overline{\gamma}_1\Gamma\left(\mu_1\right)}\right\}^{\frac{\mu_1\alpha_1}{2}}\exp\left\{\frac{\gamma_{M_i}\Gamma\left(\frac{2}{\alpha_1}+\mu_1\right)}{\overline{\gamma}_1\Gamma\left(\mu_1\right)}\right\}^{\frac{\alpha_1}{2}} \tag{1}$$

$$=A_1\left(\gamma_{M_i}\right)^{\frac{\mu_1\alpha_1}{2}-1}\mathrm{e}^{-B_1\left(\gamma_{M_i}\right)^{\frac{\alpha_1}{2}}},$$

where $A_1=\dfrac{\alpha_1}{2\Gamma\left(\mu_1\right)}\left\{\dfrac{\Gamma\left(\frac{2}{\alpha_1}+\mu_1\right)}{\overline{\gamma}_1\Gamma\left(\mu_1\right)}\right\}^{\frac{\mu_1\alpha_1}{2}}$ and $B_1=\left\{\dfrac{\Gamma\left(\frac{2}{\alpha_1}+\mu_1\right)}{\overline{\gamma}_1\Gamma\left(\mu_1\right)}\right\}^{\frac{\alpha_1}{2}}$.

3.2. PDF of Eavesdrppor's Channel

Let γ_{E_j} denotes the SNR of jth eavesdropper's channel. Then, the PDF of γ_{E_j} for MIMO OSFBC OFDM system over α-μ fading channel is given by,

$$f_{\gamma_{E_j}}\left(\gamma_{E_j}\right)=\frac{\alpha_2}{2\gamma_{E_j}\Gamma\left(\mu_2\right)}\left\{\frac{\gamma_{E_j}\Gamma\left(\frac{2}{\alpha_2}+\mu_2\right)}{\overline{\gamma}_2\Gamma\left(\mu_2\right)}\right\}^{\frac{\mu_2\alpha_2}{2}}\exp\left\{\frac{\gamma_{E_j}\Gamma\left(\frac{2}{\alpha_2}+\mu_2\right)}{\overline{\gamma}_2\Gamma\left(\mu_2\right)}\right\}^{\frac{\alpha_2}{2}} \tag{2}$$

$$=A_2\left(\gamma_{E_j}\right)^{\frac{\mu_2\alpha_2}{2}-1}\mathrm{e}^{-B_2\left(\gamma_{E_j}\right)^{\frac{\alpha_2}{2}}},$$

where $A_2 = \frac{\alpha_2}{2\Gamma(\mu_2)}\left\{\frac{\Gamma\left(\frac{2}{\alpha_2}+\mu_2\right)}{\bar{\gamma}_2\Gamma(\mu_2)}\right\}^{\frac{\mu_2\alpha_2}{2}}$ and $B_2 = \left\{\frac{\Gamma\left(\frac{2}{\alpha_2}+\mu_2\right)}{\bar{\gamma}_2\Gamma(\mu_2)}\right\}^{\frac{\alpha_2}{2}}$.

3.3. CDF of γ_{M_i}

The CDF of ith multicast channel denoted by $F_{\gamma_{M_i}}\left(\gamma_{M_i}\right)$ can be defined as

$$F_{\gamma_{M_i}}\left(\gamma_{M_i}\right) = \int_0^{\gamma_{M_i}} f_{\gamma_{M_i}}\left(\gamma_{M_i}\right)\mathrm{d}\gamma_{M_i} \tag{3}$$

Substituting the value of $f_{\gamma_{M_i}}\left(\gamma_{M_i}\right)$ in Equation (3) and performing integration we have

$$F_{\gamma_{M_i}}\left(\gamma_{M_i}\right) = A_1 A_3 \left(\gamma_{M_i}\right)^{\frac{\alpha_1}{2}(\mu_1+n)}, \tag{4}$$

where $A_3 = \sum_{n=0}^{\infty} \frac{(-1)^n (B_1)^n}{n!(\mu_1+n)\frac{\alpha_1}{2}}$.

3.4. CDF of γ_{E_j}

The CDF of jth eavesdropper's channel denoted by $F_{\gamma_{E_j}}\left(\gamma_{E_j}\right)$ can be defined as

$$F_{\gamma_{E_j}}\left(\gamma_{E_j}\right) = \int_0^{\gamma_{E_j}} f_{\gamma_{E_j}}\left(\gamma_{E_j}\right)\mathrm{d}\gamma_{E_j} \tag{5}$$

Substituting the value of $f_{\gamma_{E_j}}\left(\gamma_{E_j}\right)$ in Equation (5) and performing integration we have

$$F_{\gamma_{E_j}}\left(\gamma_{E_j}\right) = A_2 \sum_{q=0}^{\infty} \frac{(-1)^q (B_2)^q}{q!(\mu_2+q)\frac{\alpha_2}{2}} \left(\gamma_{E_j}\right)^{\frac{\alpha_2}{2}(\mu_2+q)} \tag{6}$$

3.5. PDF of Minimum SNR of Multicast Channels

Let $d_{\min} = \min_{1\le i\le M} \gamma_{M_i}$. Then, the PDF of $d_{\min}$ denoted by $f_{d_{\min}}\left(\gamma_{M_i}\right)$ can be defined as

$$f_{d_{\min}}\left(\gamma_{M_i}\right) = M f_{\gamma_{M_i}}\left(\gamma_{M_i}\right)\left\{1 - F_{\gamma_{M_i}}\left(\gamma_{M_i}\right)\right\}^{M-1} \tag{7}$$

Substituting the values of Equations (1) and (4) into Equation (7) and performing integration we have

$$\begin{aligned} f_{d_{\min}}\left(\gamma_{M_i}\right) = MA_1 \Bigg[& \gamma_{M_i}^{\frac{\mu_1\alpha_1}{2}-1} - (M-1)A_1A_3 \\ & \times \left\{ \gamma_{M_i}^{\frac{v_{m_1}}{2}-1} - \frac{(M-2)A_1A_3}{2!}\gamma_{M_i}^{\frac{v_{m_2}}{2}-1} \right\} \Bigg] \mathrm{e}^{-B_1\gamma_{M_i}^{\frac{\alpha_1}{2}}} \end{aligned} \tag{8}$$

where $A_3 = \sum_{n=0}^{\infty} \frac{(-1)^n (B_1)^n}{n!(\mu_1+n)\frac{\alpha_1}{2}}$, $v_{m_1} = 2\mu_1\alpha_1 + n\alpha_1$ and $v_{m_2} = 3\mu_1\alpha_1 + 2n\alpha_1$.

3.6. PDF of Maximum SNR of Eavesdropper's Channels

Let $d_{\max} = \max_{1\le j\le N} \gamma_{E_j}$. Then, the PDF of $d_{\max}$ denoted by $f_{d_{\max}}\left(\gamma_{E_j}\right)$ can be defined as

$$f_{d_{\max}}\left(\gamma_{E_j}\right) = N f_{\gamma_{E_j}}\left(\gamma_{E_j}\right)\left\{F_{\gamma_{E_j}}\left(\gamma_{E_j}\right)\right\}^{N-1} \tag{9}$$

Substituting the values of Equations (2) and (6) into Equation (9) and performing integration we have

$$f_{d_{\max}}\left(\gamma_{E_j}\right) = \frac{NA_2A_4\left\{c_0\gamma_{E_j}^{\frac{v_{e_3}}{2}-1} + c_1\gamma_{E_j}^{\frac{v_{e_4}}{2}-1}\right\}}{\mathrm{e}^{B_2\left(\gamma_{E_j}\right)^{\frac{\alpha_2}{2}}}}, \tag{10}$$

where

$$A_4 = \left(\frac{2A_2}{\alpha_2}\right)^{N-1}, c_0 = \left(\frac{1}{\mu_2}\right)^{N-1}, c_1 = \frac{(N-1)(\mu_2)^{2-N}(-B_2)}{\mu_2+1},$$
$$v_{e_1} = N\mu_2\alpha_2 - \mu_2\alpha_2, v_{e_2} = N\mu_2\alpha_2 - \mu_2\alpha_2 + \alpha_2,$$
$$v_{e_3} = v_{e_1} + \mu_2\alpha_2, v_{e_4} = v_{e_2} + \mu_2\alpha_2.$$

4. Probability of Non-Zero Secrecy Multicast Capacity

The probability of non-zero secrecy multicast capacity denoted by $Pr\left(C_{smcast} > 0\right)$ can be defined as

$$Pr\left(C_{smcast} > 0\right) = \int_0^\infty f_{d_{\min}}\left(\gamma_{M_i}\right)\left\{\int_0^{\gamma_{M_i}} f_{d_{\max}}\left(\gamma_{E_j}\right)\mathrm{d}\gamma_{E_j}\right\}\mathrm{d}\gamma_{M_i} \tag{11}$$

Substituting the values of $f_{d_{\min}}\left(\gamma_{M_i}\right)$ and $f_{d_{\max}}\left(\gamma_{E_j}\right)$ in Equation (11) and performing integration, the closed-form analytical expression for the $Pr\left(C_{smcast} > 0\right)$ is given in Equation (12) at the bottom of this page,

$$\begin{aligned} &Pr\left(C_{smcast} > 0\right) \\ &= \frac{MA_1}{\frac{\alpha_1}{2}}\left\{\frac{A_5\Gamma\left(\frac{v_{p_1}}{\alpha_1}\right)}{B_1^{\frac{v_{p_1}}{\alpha_1}}} + \frac{A_6\Gamma\left(\frac{v_{p_2}}{\alpha_1}\right)}{B_1^{\frac{v_{p_2}}{\alpha_1}}}\right\} - M(M-1)A_1^2A_3\left\{A_5\frac{\Gamma\left(\frac{v_{p_3}}{\alpha_1}\right)}{\frac{\alpha_1}{2}B_1^{\frac{v_{p_3}}{\alpha_1}}} - A_6\frac{\Gamma\left(\frac{v_{p_4}}{\alpha_1}\right)}{\frac{\alpha_1}{2}B_1^{\frac{v_{p_4}}{\alpha_1}}}\right\} \\ &+ \frac{M(M-1)(M-2)A_1^3A_3^2}{2!}\left\{A_5\frac{\Gamma\left(\frac{v_{p_5}}{\alpha_1}\right)}{\frac{\alpha_1}{2}B_1^{\frac{v_{p_5}}{\alpha_1}}} + A_6\frac{\Gamma\left(\frac{v_{p_6}}{\alpha_1}\right)}{\frac{\alpha_1}{2}B_1^{\frac{v_{p_6}}{\alpha_1}}}\right\}, \end{aligned} \tag{12}$$

where

$$A_5 = \frac{Nc_0A_2A_4}{\frac{\alpha_2}{2}}\sum_{n_1=0}^{\infty}\frac{(-1)^{n_1}B_2^{n_1}}{n_1!\left(\frac{v_{e_3}}{\alpha_2}+n_1\right)}, v_{e_5} = v_{e_3} + n_1\alpha_2, v_{e_6} = v_{e_4} + n_2\alpha_2,$$

$$A_6 = \frac{Nc_1 A_2 A_4}{\frac{\alpha_2}{2}} \sum_{n_2=0}^{\infty} \frac{(-1)^{n_2} B_2^{n_2}}{n_2 ! \left(\frac{v_{e_4}}{\alpha_2} + n_2 \right)}, v_{p_1} = \mu_1 \alpha_1 + v_{e_5}, v_{p_2} = \mu_1 \alpha_1 + v_{e_6},$$

$$v_{p_3} = v_{m_1} + v_{e_5}, v_{p_4} = v_{m_1} + v_{e_6}, v_{p_5} = v_{m_2} + v_{e_5}, v_{p_6} = v_{m_2} + v_{e_6}.$$

5. Secure Outage Probability for Multicasting

The secure outage probability for multicasting denoted by $P_{out}\left(R_{smcast}\right)$ can be defined as

$$P_{out}\left(R_{smcast}\right) = 1 - \int_0^{\infty} f_{d_{\max}}\left(\gamma_{E_j}\right) \left\{ \int_x^{\infty} f_{d_{\min}}\left(\gamma_{M_i}\right) \mathrm{d}\gamma_{M_i} \right\} \mathrm{d}\gamma_{E_j}, \tag{13}$$

where $x = \mathrm{e}^{2R_{smcast}}\left(1+\gamma_j\right) - 1$ and R_{smcast} denotes the target secrecy multicast rate. Now, substituting the values of $f_{d_{\min}}\left(\gamma_{M_i}\right)$ in Equation (13) and performing integration the closed-form analytical expression for $P_{out}\left(R_{smcast}\right)$ is given in Equation (14) at the bottom of the next page,

$$\begin{aligned} P_{out}\left(R_{smcast}\right) = 1 - \frac{MNA_1 A_2 A_4}{\frac{\alpha_2}{2}} \Bigg[& A_7 A_8 \left\{ \frac{c_0 \Gamma\left(\frac{u_{e_1}}{\alpha_2}\right)}{\left(B_3\right)^{\frac{u_{e_1}}{\alpha_2}}} + \frac{c_1 \Gamma\left(\frac{u_{e_4}}{\alpha_2}\right)}{\left(B_3\right)^{\frac{u_{e_4}}{\alpha_2}}} \right\} \\ & - A_1 A_3 A_{10} A_{11} \left\{ \frac{c_0 \Gamma\left(\frac{u_{e_2}}{\alpha_2}\right)}{\left(B_3\right)^{\frac{u_{e_2}}{\alpha_2}}} + \frac{c_1 \Gamma\left(\frac{u_{e_5}}{\alpha_2}\right)}{\left(B_3\right)^{\frac{u_{e_5}}{\alpha_2}}} \right\} \\ & + A_1^2 A_3^2 A_{12} A_{13} \left\{ \frac{c_0 \Gamma\left(\frac{u_{e_3}}{\alpha_2}\right)}{\left(B_3\right)^{\frac{u_{e_3}}{\alpha_2}}} + \frac{c_1 \Gamma\left(\frac{u_{e_6}}{\alpha_2}\right)}{\left(B_3\right)^{\frac{u_{e_6}}{\alpha_2}}} \right\} \Bigg] \end{aligned} \tag{14}$$

where

$$A_7 = \frac{2\frac{(M-1)!}{0!(M-1)!}}{\alpha_1 B_1^{\mu_1}} \Gamma\left(\mu_1\right) \sum_{m_1=0}^{\mu_1 - 1} \frac{B_1^{m_1}}{m_1 !},$$

$$A_8 = \sum_{n_3=0}^{\frac{m_1 \alpha_1}{2}} \frac{\left(\frac{m_1 \alpha_1}{2}\right)!}{n_3 ! \left(\frac{m_1 \alpha_1}{2} - n_3\right)!} \frac{\left(\mathrm{e}^{2R_s} - 1\right)^{n_3}}{\left(\mathrm{e}^{2R_s}\right)^{n_3 - \frac{m_1 \alpha_1}{2}}},$$

$$A_9 = \sum_{n_4=0}^{\frac{\alpha_1}{2}} \frac{\left(\frac{\alpha_1}{2}\right)!}{n_4 ! \left(\frac{\alpha_1}{2} - n_4\right)!} \frac{\left(\mathrm{e}^{2R_s} - 1\right)^{n_4}}{\left(\mathrm{e}^{2R_s}\right)^{n_4 - \frac{\alpha_1}{2}}},$$

$$A_{10} = \frac{2\frac{(M-1)!}{1!(M-2)!}}{\alpha_1 B_1^{\frac{v_{m_1}}{\alpha_1}}} \Gamma\left(\frac{v_{m_1}}{\alpha_1}\right) \sum_{m_2=0}^{\frac{v_{m_1}}{\alpha_1} - 1} \frac{B_1^{m_2}}{m_2 !},$$

$$A_{11}=\sum_{n_5=0}^{\frac{m_2\alpha_1}{2}}\frac{\frac{m_2\alpha_1}{2}!}{n_5!\left(\frac{m_2\alpha_1}{2}-n_5\right)!}\frac{\left(e^{2R_s}-1\right)^{n_5}}{\left(e^{2R_s}\right)^{n_5-\frac{m_2\alpha_1}{2}}},$$

$$A_{12}=\frac{2\frac{(M-1)!}{2!(M-3)!}\Gamma\left(\frac{v_{m_2}}{\alpha_1}\right)\sum_{m_3=0}^{\frac{v_{m_2}}{\alpha_1}-1}\frac{B_1^{m_3}}{m_3!}}{\alpha_1 B_1^{\frac{v_{m_2}}{\alpha_1}}},$$

$$A_{13}=\sum_{n_6=0}^{\frac{m_3\alpha_1}{2}}\frac{\frac{m_3\alpha_1}{2}!}{n_6!\left(\frac{m_3\alpha_1}{2}-n_6\right)!}\frac{\left(e^{2R_s}-1\right)^{n_6}}{\left(e^{2R_s}\right)^{n_6-\frac{m_3\alpha_1}{2}}},$$

$$u_{e_1}=v_{e_3}+m_1\alpha_1-2n_3, u_{e_2}=v_{e_3}+m_2\alpha_1-2n_5, u_{e_3}=v_{e_3}+m_3\alpha_1-2n_6,$$

$$u_{e_4}=v_{e_4}+m_1\alpha_1-2n_3, u_{e_5}=v_{e_4}+m_2\alpha_1-2n_5$$

and

$$u_{e_6}=v_{e_4}+m_3\alpha_1-2n_6.$$

6. Numerical Results

Figure 2 shows the probability of non-zero secrecy multicast capacity, $Pr\left(C_{smcast}>0\right)$, as a function of the average SNR of the multicast channel, $\overline{\gamma}_M$, for selected values of M and N. This figure describes the effects of M and N on the $Pr\left(C_{smcast}>0\right)$ for selected values of system parameters. We see that the $Pr\left(C_{smcast}>0\right)$ decreases, if the number of eavesdropper, N, increases from 1 to 2. $Pr\left(C_{smcast}>0\right)$ decreases, if the number of multicast user, M, increases from 1 (indicated by the long-dash line and solid line) to 2 (indicated by the short-dash line and dotted line) with the system parameters $\alpha_m=0.6$, $\alpha_e=1$, $\mu_m=1.5$, $\mu_e=1$ and $\gamma_e=20$ dB. This is because, in the multicast channel, increasing in the number of multicast user reduces the bandwidth of each user which causes a reduction in the capacity of each multicast user. In the eavesdropper channel, increasing in the number of eavesdropper increases the probability of eavesdropping and causes a reduction in the secrecy capacity.

Figure 3 shows the $Pr\left(C_{smcast}>0\right)$, as a function of $\overline{\gamma}_M$, for selected values of the average SNR of eavesdropper channel, $\overline{\gamma}_e$. This figure describes the effects of $\overline{\gamma}_e$ on the $Pr\left(C_{smcast}>0\right)$ for selected values of system parameters. We see that $Pr\left(C_{smcast}>0\right)$ decreases with γ_e increases. Because, the capacity of eavesdropper's channel increases with γ_e which causes a reduction in the secrecy capacity.

Figure 4 shows the $Pr\left(C_{smcast}>0\right)$, as a function of $\overline{\gamma}_M$ for selected values of the arbitrary constant, α_m and M. This figure describes the effects of α_m on the $Pr\left(C_{smcast}>0\right)$ for the selected values of system parameters. We see that the $Pr\left(C_{smcast}>0\right)$ increases with α_m for different values of M. This is because, the capacity of multicast channel increases with α_m which causes an improvement in the secrecy capacity.

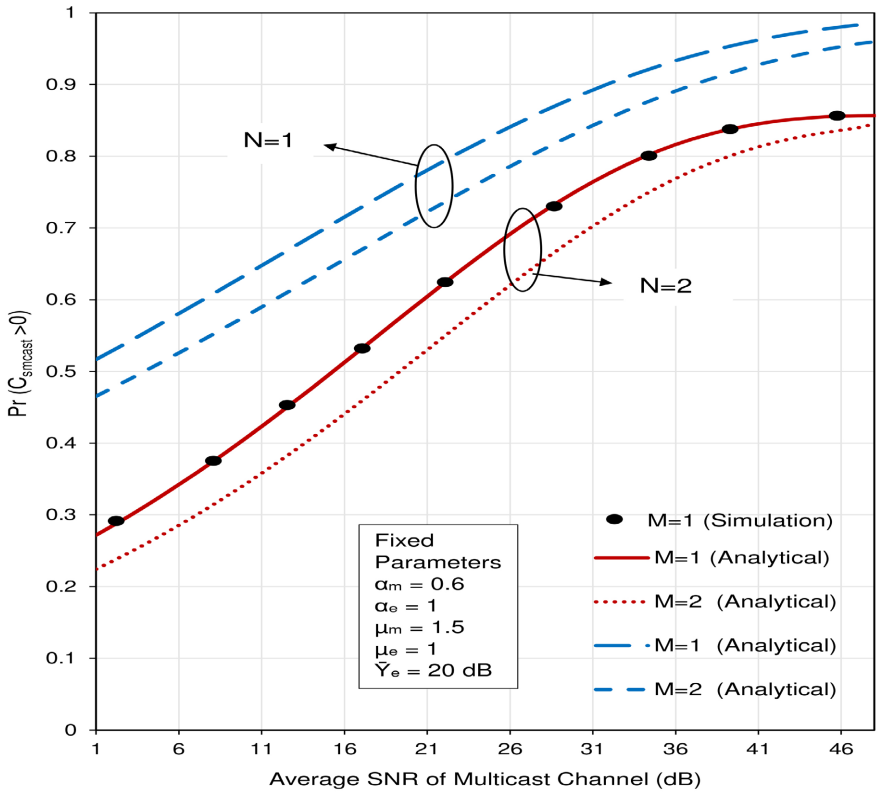

Figure 2. The effects of the number of multicast user, *M*, and eavesdropper, *N*, on the $Pr\left(C_{smcast}>0\right)$ with $\alpha_m=0.6$, $\alpha_e=1$, $\mu_m=1.5$, $\mu_e=1$ and $\gamma_e=20\,\text{dB}$.

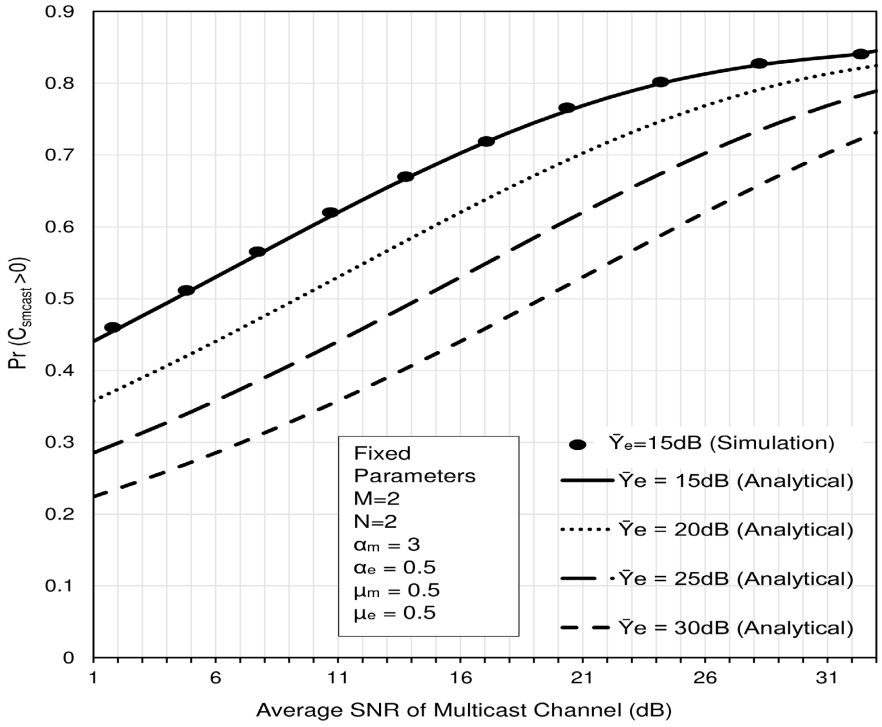

Figure 3. The effect of average SNR of eavesdropper's channel, γ_e, on the $Pr\left(C_{smcast}>0\right)$ for $M=2$, $N=2$, $\alpha_m=3$, $\alpha_e=0.5$, $\mu_m=0.5$ and $\mu_e=0.5$.

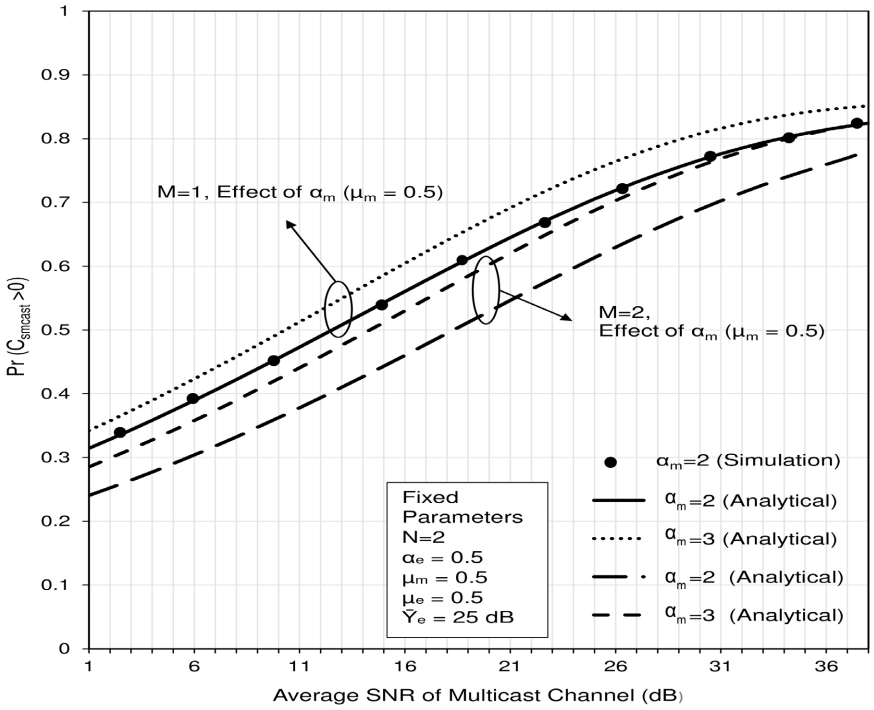

Figure 4. The effect of arbitrary constant, α_m, on the $Pr(C_{smcast}>0)$ for selected values of M with $N=2$, $\alpha_e=0.5$, $\mu_m=0.5$, $\mu_e=0.5$ and $\gamma_e=25$ dB.

Figure 5 shows the $Pr(C_{smcast}>0)$, as a function of $\overline{\gamma}_M$ for selected values of the arbitrary constant μ_m and M. This figure describes the effect of μ_m on the $Pr(C_{smcast}>0)$ for selected values of system parameters. We see that the $Pr(C_{smcast}>0)$ increases with μ_m for different values of M. This is because, the capacity of multicast channel increases with μ_m which causes an improvement in the secrecy capacity.

Figure 6 shows the $Pr(C_{smcast}>0)$, as a function of the $\overline{\gamma}_M$ for selected values of the arbitrary constant α_e and M. This figure describes the effects of α_e on the $Pr(C_{smcast}>0)$ for selected values of system parameters. We see that the $Pr(C_{smcast}>0)$ decreases with α_e for different values of M. This is because, the capacity of eavesdropper's channel increases with α_e which causes a reduction in the secrecy capacity.

Figure 7 shows the $Pr(C_{smcast}>0)$, as a function of $\overline{\gamma}_M$ for selected values of the arbitrary constant μ_e and M. This figure describes the effects of μ_e on the $Pr(C_{smcast}>0)$ for selected values of system parameters. We see that the $Pr(C_{smcast}>0)$ decreases with μ_e for different values of M. This is because, the capacity of eavesdropper's channel increases with μ_e which causes a reduction in the secrecy capacity.

Figure 8 shows the $Pr(C_{smcast}>0)$, as a function of the $\overline{\gamma}_M$ for selected values of the arbitrary constant α_m and N. This figure describes the effects of α_m for selected values of N on the $Pr(C_{smcast}>0)$ for selected values of system parameters. We see that the $Pr(C_{smcast}>0)$ increases with α_m for different values of N but decreases with N.

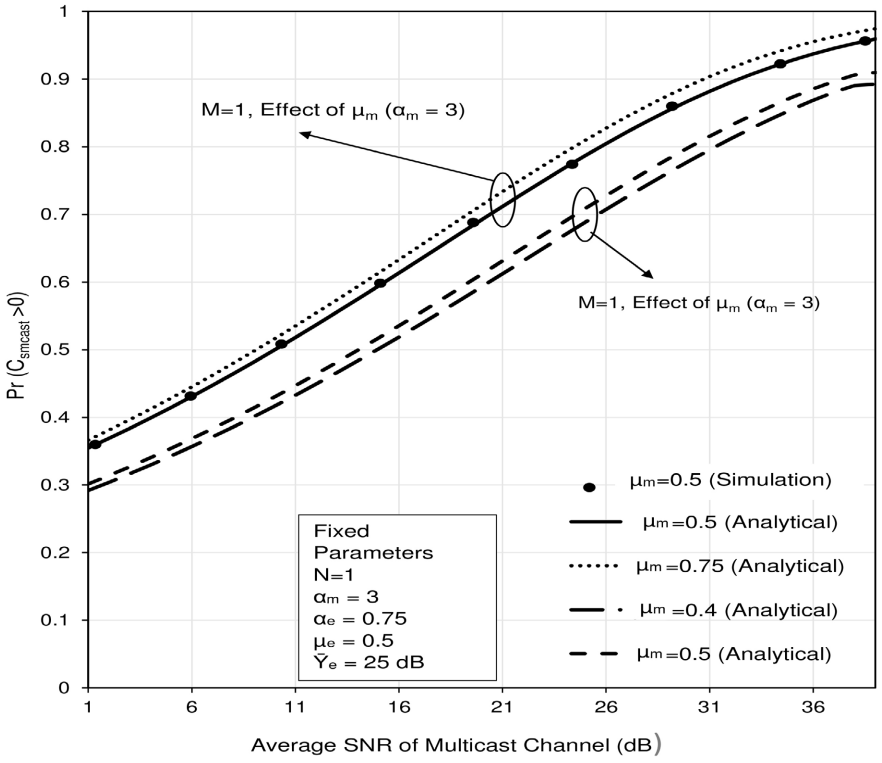

Figure 5. The effect of arbitrary constant, μ_m, on the $Pr(C_{smcast}>0)$ for selected values of M with $N=1$, $\alpha_m=3$, $\alpha_e=0.75$, $\mu_e=0.5$ and $\gamma_e=25$ dB.

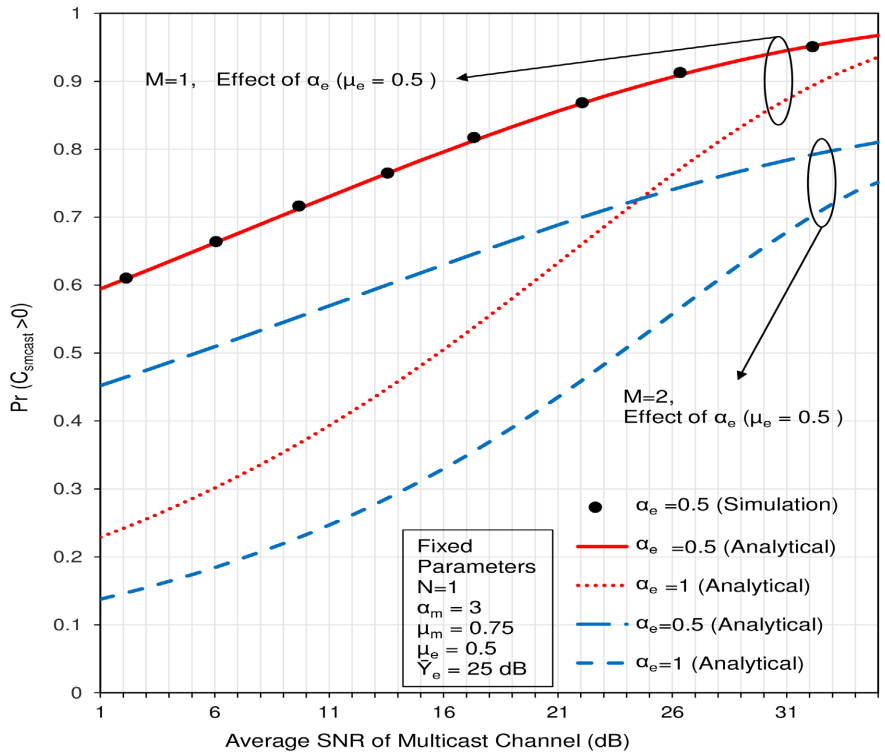

Figure 6. The effect of arbitrary constant, α_e, on the $Pr(C_{smcast}>0)$ for selected values of M with $N=1$, $\alpha_m=3$, $\mu_m=0.75$, $\mu_e=0.5$ and $\gamma_e=25$ dB.

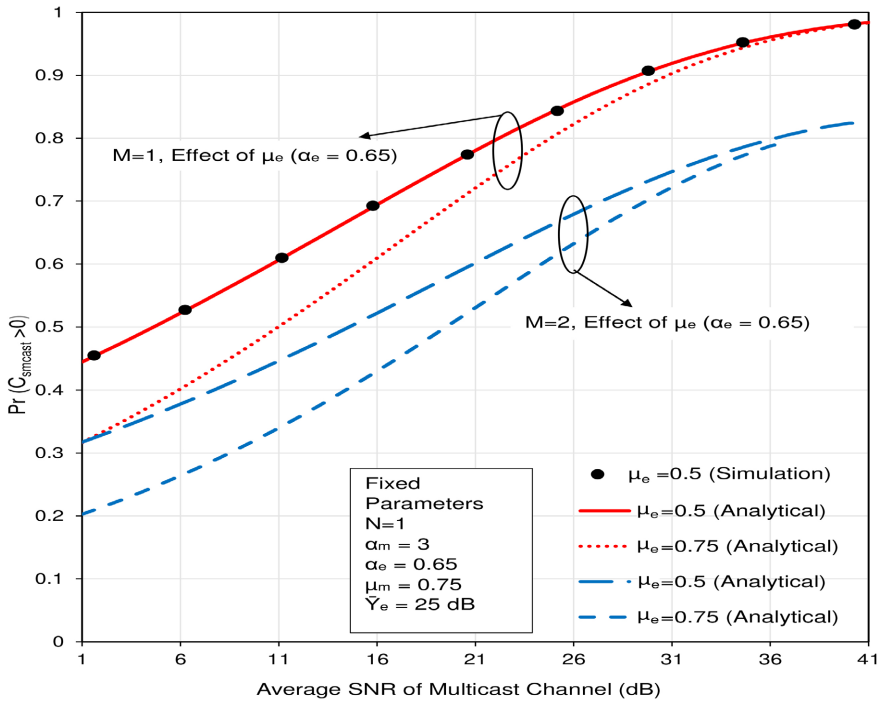

Figure 7. The effect of arbitrary constant, μ_e, on the $Pr(C_{smcast}>0)$ for selected values of M with $N=1$, $\alpha_m=3$, $\alpha_e=0.65$, $\mu_m=0.75$ and $\gamma_e=25$ dB.

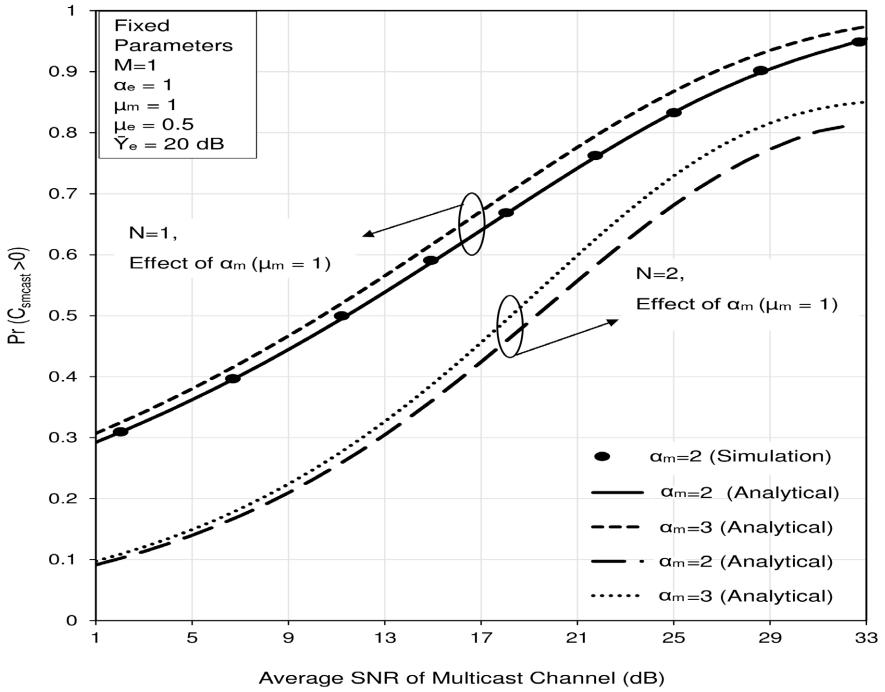

Figure 8. The effect of arbitrary constant, α_m, on the $Pr(C_{smcast}>0)$ for selected values of N with $M=1$, $\alpha_e=1$, $\mu_m=1$, $\mu_e=0.5$, $\gamma_e=20$ dB.

Figure 9 shows the $Pr(C_{smcast}>0)$, as a function of $\overline{\gamma}_M$ for selected values of the arbitrary constant, μ_m, and N. This figure describes the effects of

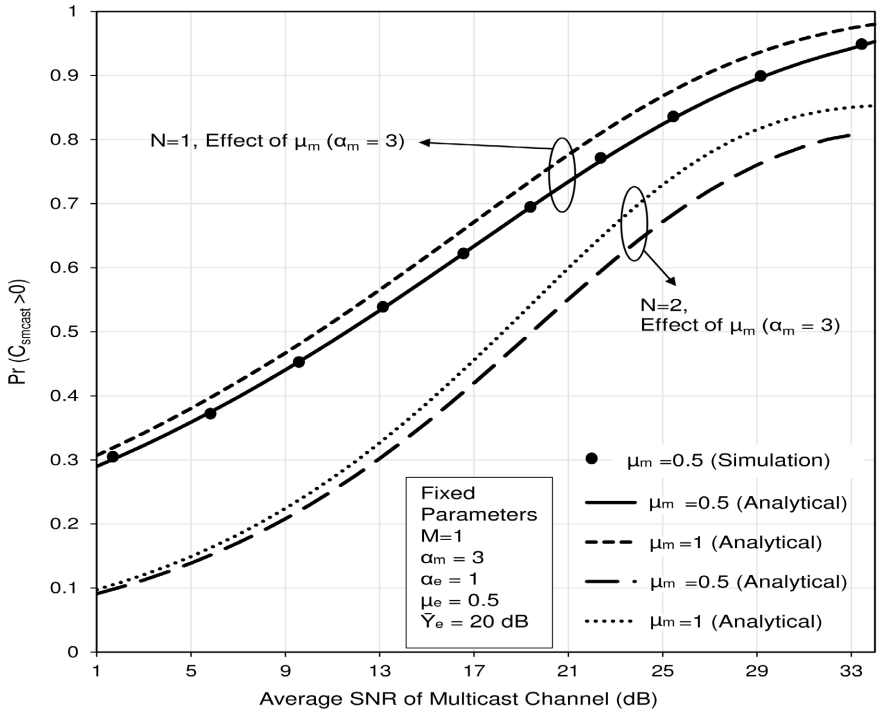

Figure 9. The effect of arbitrary constant, μ_m, on the $Pr(C_{smcast}>0)$ for selected values of N with $M=1$, $\alpha_m=3$, $\alpha_e=1$, $\mu_e=0.5$ and $\gamma_e=20$ dB.

μ_m on the $Pr(C_{smcast}>0)$ for selected values of system parameters. We see that the $Pr(C_{smcast}>0)$ increases with μ_m for different values of N but decreases with N.

Figure 10 shows the $Pr(C_{smcast}>0)$, as a function of $\overline{\gamma}_M$ for selected values of the arbitrary constant, α_e, and N. This figure describes the effects of α_e on the $Pr(C_{smcast}>0)$ for selected values of system parameters. We see that the $Pr(C_{smcast}>0)$ decreases with α_e and N.

Figure 11 shows the $Pr(C_{smcast}>0)$, as a function of $\overline{\gamma}_M$ for selected values of the arbitrary constant μ_e and N. This figure describes the effects of μ_e on the $Pr(C_{smcast}>0)$ for selected values of system parameters. We see that the $Pr(C_{smcast}>0)$ decreases with μ_e.

Figure 12 shows the outage probability for multicasting, $P_{out}(R_{smcast})$, as a function of $\overline{\gamma}_M$ for selected values of the number of eavesdropper, N. This figure describes the effects of N on the $P_{out}(R_{smcast})$ for selected values of system parameters. It is observed that the $P_{out}(R_{smcast})$ increases with N increases. This is because, the increases in the number of eavesdroppers increases the probability of eavesdropping and decreases the secrecy capacity which causes an improvement in the $P_{out}(R_{smcast})$.

Figure 13 shows the $P_{out}(R_{smcast})$, as a function of $\overline{\gamma}_M$ for selected values of $\overline{\gamma}_e$. This figure describes the effects of $\overline{\gamma}_e$ on the $P_{out}(R_{smcast})$ for selected values of system parameters. We see that the $P_{out}(R_{smcast})$ increases if the value of $\overline{\gamma}_e$ increases. This is because, the increases in $\overline{\gamma}_e$ increases the capacity

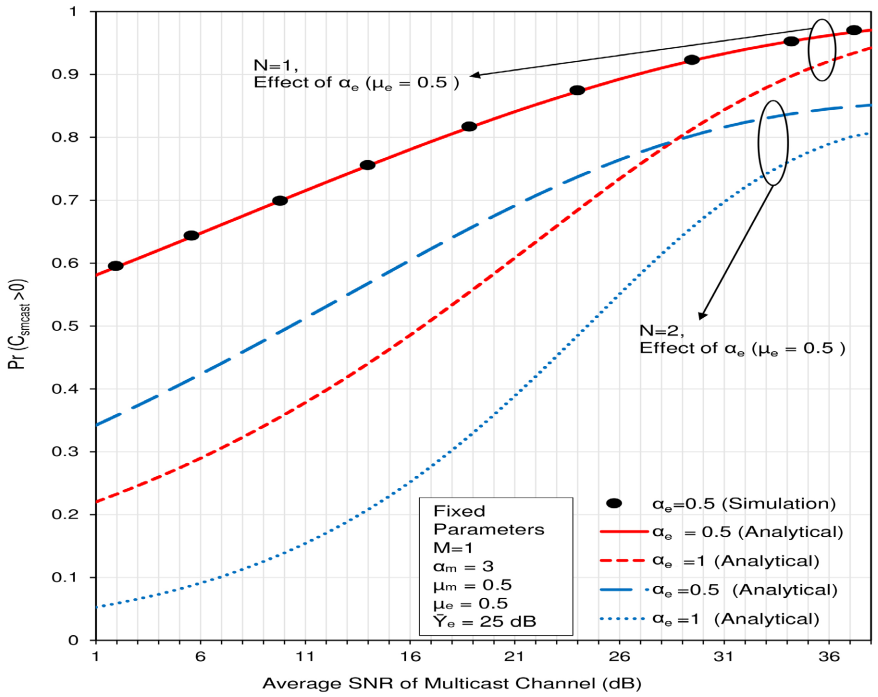

Figure 10. The effect of arbitrary constant, α_e, on the $Pr(C_{smcast} > 0)$ for selected values of N with $M = 1$, $\alpha_m = 3$, $\mu_m = 0.5$, $\mu_e = 0.5$ and $\gamma_e = 25$ dB.

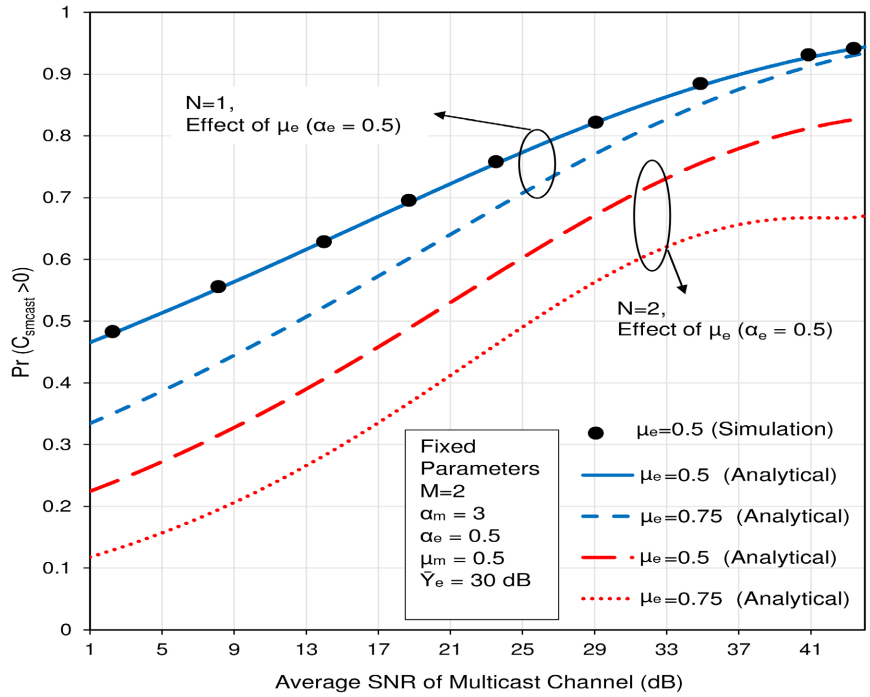

Figure 11. The effect of arbitrary constant, μ_e, on the $Pr(C_{smcast} > 0)$ for selected values of N with $M = 2$, $\alpha_m = 3$, $\alpha_e = 0.5$, $\mu_m = 0.5$ and $\gamma_e = 30$ dB.

of eavesdropper's channel and decreases the secrecy capacity which causes an improvement in the $P_{out}(R_{smcast})$.

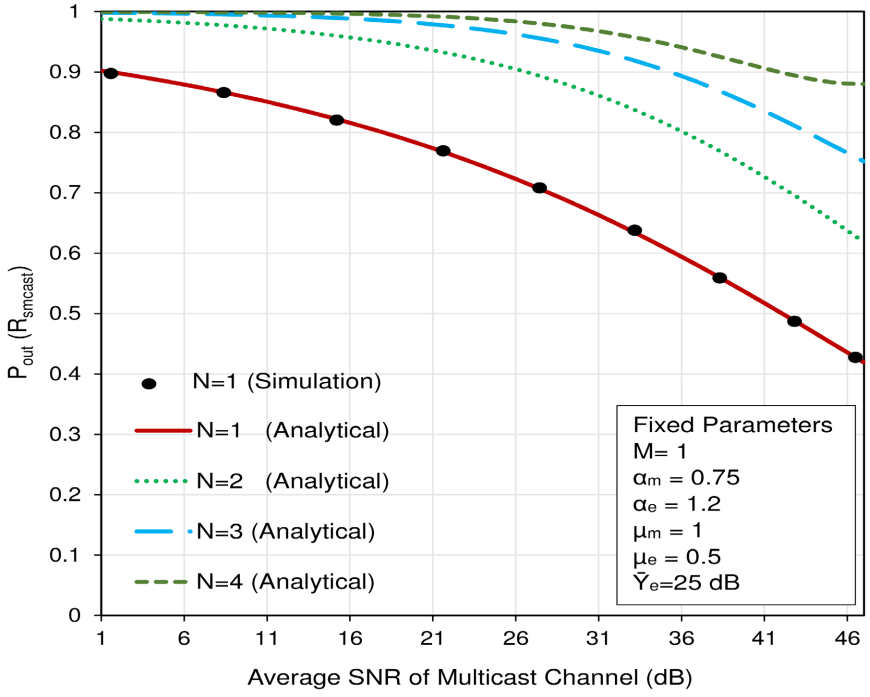

Figure 12. The effect of number of eavesdropper, N, on the $P_{out}\left(R_{smcast}\right)$ for $M=1$, $\alpha_m=0.75$, $\alpha_e=1.2$, $\mu_m=1$, $\mu_e=0.5$, $\gamma_e=25\,\text{dB}$ and $R_{smcast}=0.5$.

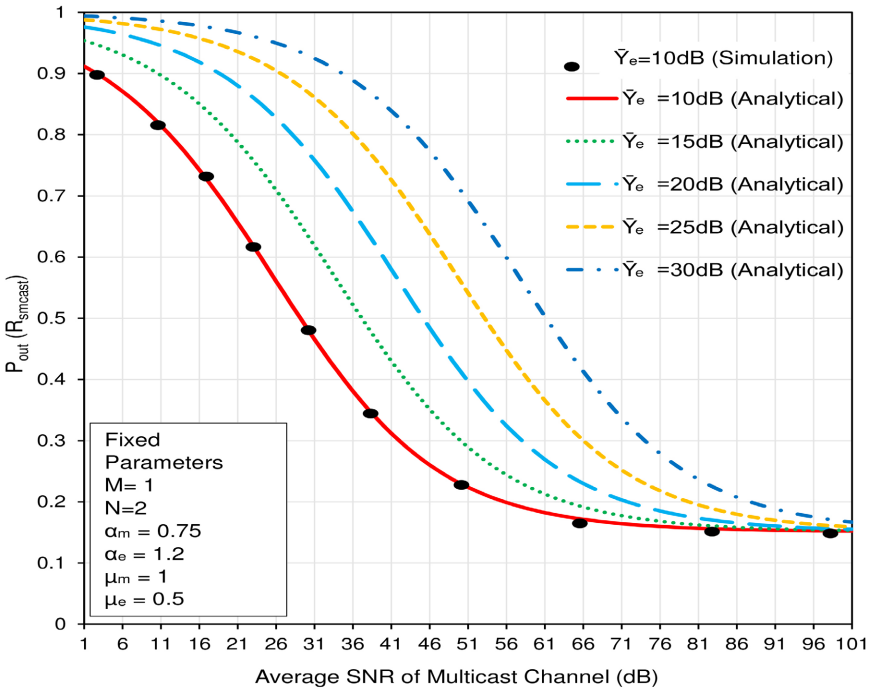

Figure 13. The effect of average SNR of eavesdropper's channel, γ_e, on the $P_{out}\left(R_{smcast}\right)$ for $M=1$, $N=2$, $\alpha_m=0.75$, $\alpha_e=1.2$, $\mu_m=1$, $\mu_e=0.5$, $R_{smcast}=0.5$.

Figure 14 shows the $P_{out}\left(R_{smcast}\right)$, as a function of $\overline{\gamma}_M$ for selected values of the arbitrary constant α_m and N. This figure describes the effects of α_m

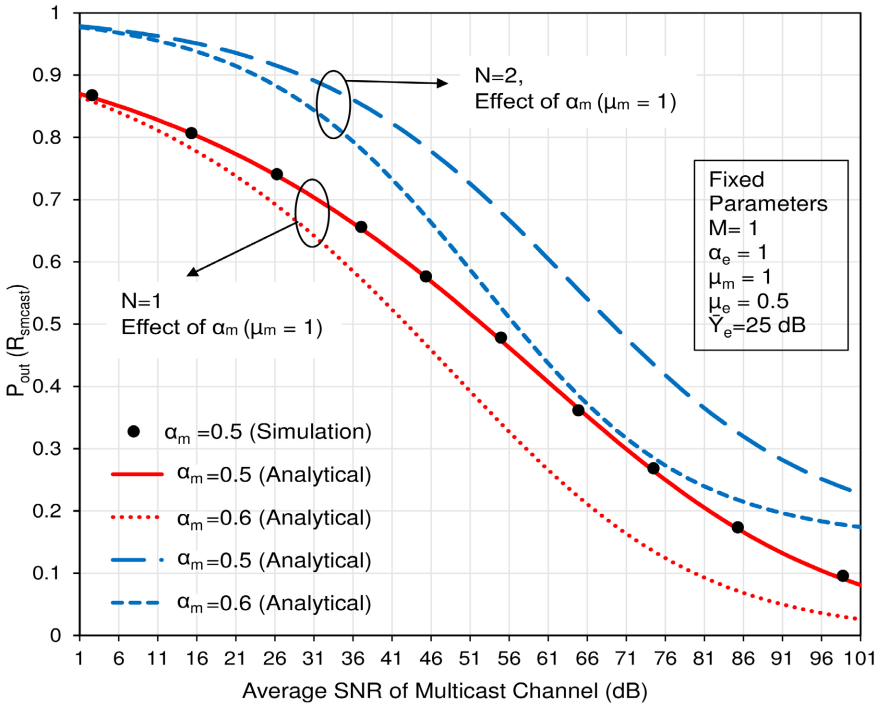

Figure 14. The effect of arbitrary constant, α_m, on the $P_{out}(R_{smcast})$ for selected values of N with $M=1$, $\alpha_e=1$, $\mu_m=1$, $\mu_e=0.5$, $R_{smcast}=0.5$ and $\gamma_e=25$ dB.

on the $P_{out}(R_{smcast})$ for selected values of system parameters. We see that for different selected values of N the $P_{out}(R_{smcast})$ decreases if α_m increases. This is because, the capacity of multicast channel increases with α_m and enhances the secrecy capacity which causes a reduction in the secure outage probability.

Figure 15 shows the $P_{out}(R_{smcast})$, as a function of $\overline{\gamma}_M$ for selected values of the arbitrary constant μ_m and N. This figure describes the effects of μ_m on the $P_{out}(R_{smcast})$ for selected values of system parameters. We see that for different selected values of N the $P_{out}(R_{smcast})$ decreases if μ_m increases. This is because, the capacity of multicast channel increases with μ_m and improves the secrecy capacity which causes a reduction in the secure outage probability.

Figure 16 shows the $P_{out}(R_{smcast})$, as a function of $\overline{\gamma}_M$ for selected values of the arbitrary constant α_e and N. This figure describes the effects of α_e on the $P_{out}(R_{smcast})$ for selected values of system parameters. We see that for different selected values of N the $P_{out}(R_{smcast})$ increases with α_e as one expects.

Figure 17 shows the $P_{out}(R_{smcast})$, as a function of $\overline{\gamma}_M$ for selected values of the arbitrary constant μ_e and N. This figure describes the effects of μ_e on the $P_{out}(R_{smcast})$ for selected values of system parameters. We see that for different selected values of N the $P_{out}(R_{smcast})$ increases with μ_e as one expects.

Therefore, based on the closed-form analytical expressions for the $Pr(C_{smcast}>0)$ and the $P_{out}(R_{smcast})$, and from the observations of numerical results, the main findings of this paper can be summarized as follows: The increase in γ_e, M, N, α_e and μ_e degrades the security of the proposed system.

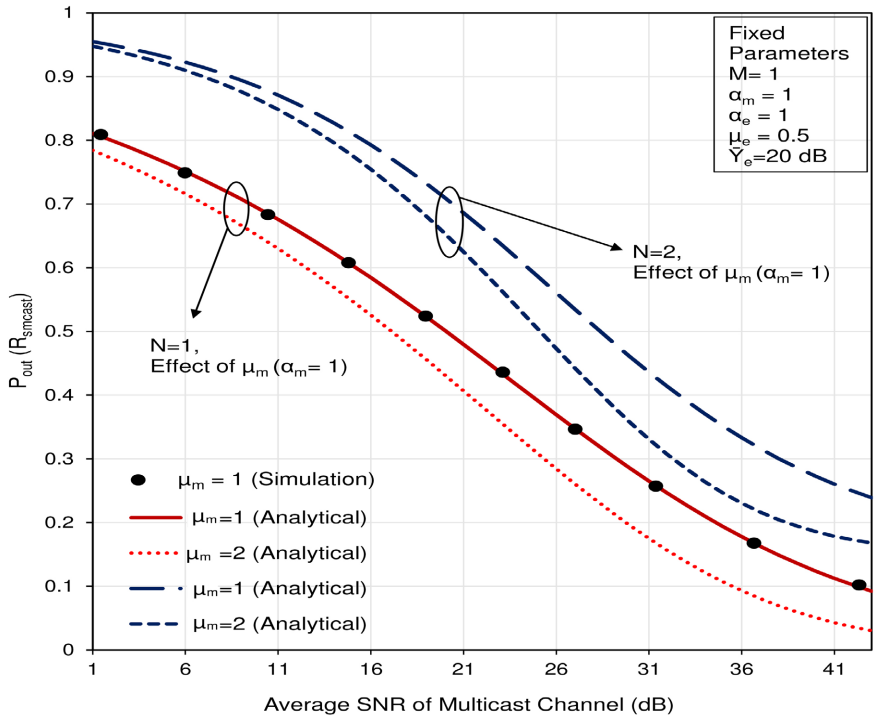

Figure 15. The effect of arbitrary constant, μ_m, on the $P_{out}(R_{smcast})$ for selected values of N with $M=1$, $\alpha_m=1$, $\alpha_e=1$, $\mu_e=0.5$, $R_{smcast}=0.5$ and $\gamma_e=20$ dB.

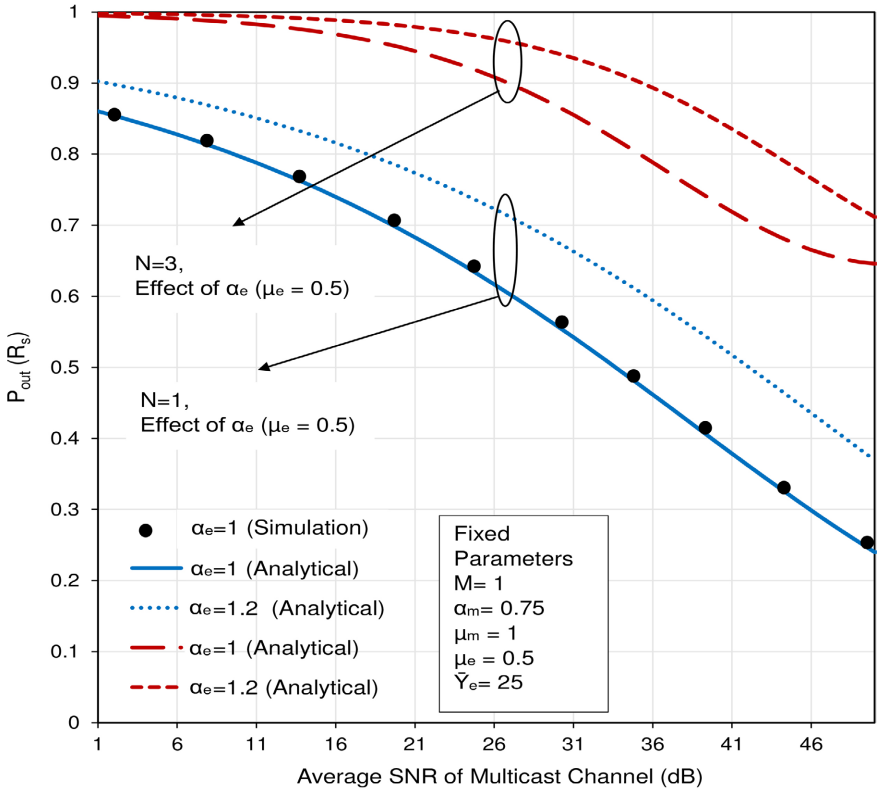

Figure 16. The effect of arbitrary constant, α_e, on the $P_{out}(R_{smcast})$ for selected values of N with $M=1$, $\alpha_e=0.75$, $\mu_m=1$, $\mu_e=0.5$, $R_{smcast}=0.5$ and $\gamma_e=25$ dB.

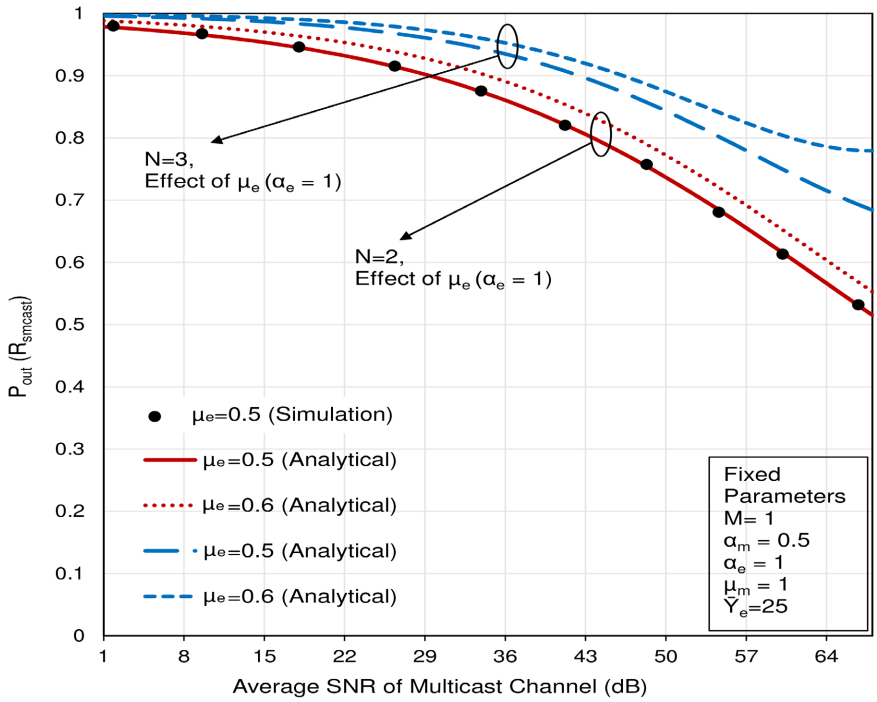

Figure 17. The effect of arbitrary constant, μ_e, on the $P_{out}\left(R_{smcast}\right)$ for selected values of N with $M=1$, $\alpha_m=0.5$, $\alpha_e=1$, $\mu_m=1$, $R_{smcast}=0.5$ and $\gamma_e=25$ dB.

But the increase in α_m and μ_m enhances the security of the proposed system.

7. Conclusion

This paper focuses on the development of an analytical mathematical model to ensure the security in wireless multicasting through MIMO OSFBC OFDM system over α-μ fading channel. The validity of analytical expressions is verified via Monte-Carlo simulation. The developed analytical model helps to realize the insight of the effects of system parameters such as α, μ, the number of multicast users and eavesdroppers on the security in wireless multicasting over α-μ fading channel employing OSFBC OFDM system. The observations of numerical results demonstrate that the security in α-μ fading channel is significantly affected by the fading parameters α and μ, and the number of multicast users and eavesdroppers. The increase in α and μ of main channel enhances the security. But the increase in α and μ of eavesdropper channel, and the number of multicast users and eavesdroppers degrade the security. The effects of α and μ increase in the high SNR region of the main channel. Therefore, the observations of this paper pave the way for enhancing security in the α-μ fading channels compensating the effects of aforementioned parameters with opportunistic relaying technique.

Conflicts of Interest

The authors declare no conflicts of interest regarding the publication of this paper.

References

[1] Raj, U. and Bhaskar, V. (2013) Performance Analysis of Scheduling Schemes for MIMO OSFBC-OFDM System in α-μ Fading Channel Scenarios. 2013 *International Conference on Communication and Signal Processing*, Melmaruvathur, India, 3-5 April 2013, 144-148. https://doi.org/10.1109/iccsp.2013.6577033

[2] Sarker, D.K., Sarkar, M.Z.I. and Anower, M.S. (2017) Secure Wireless Multicasting with Linear Equalization. *Physical Communication*, **25**, 201-213. https://doi.org/10.1016/j.phycom.2017.07.007

[3] Mathur, A., Ai, Y., Cheffena, M. and Kaddoum, G. (2019) Secrecy Performance of Correlated α-μ Fading Channels. *IEEE Communications Letters*, **23**, 1323-1327. https://doi.org/10.1109/LCOMM.2019.2920347

[4] Moualeu, J.M., da Costa, D.B., Lopez-Martinez, F.J., Hamouda, W., Ngatched, T.M. and Dias, U.S. (2019) Secrecy Analysis of a TAS/MRC Scheme in α-μ Fading Channels. *2019 IEEE Wireless Communications and Networking Conference* (*WCNC*). Marrakesh, Morocco, 15-18 April 2019, 1-6. https://doi.org/10.1109/WCNC.2019.8886042

[5] Moualeu, J.M., da Costa, D.B., Lopez-Martinez, F.J., Hamouda, W., Nkouatchah, T.M. and Dias, U.S. (2019) Transmit Antenna Selection in Secure MIMO Systems over α-μ Fading Channels. *IEEE Transactions on Communications*, **67**, 6483-6498. https://doi.org/10.1109/TCOMM.2019.2921966

[6] Hanif, A., Badrudduza, A., Hossen, M., Kundu, M. and Sarkar, M. (2019) Secure Outage Performance Analysis of Multicasting through α-μ Fading Channel. 2019 3*rd International Conference on Electrical*, *Computer & Telecommunication Engineering* (*ICECTE*), Rajshahi, Bangladesh, 26-28 December 2019, 65-68. https://doi.org/10.1109/ICECTE48615.2019.9303574

[7] Yadav, S. (2020) Secrecy Performance of Cognitive Radio Sensor Networks over α-μ Fading Channels. *IEEE Sensors Letters*, **4**, 1-4. https://doi.org/10.1109/LSENS.2020.3014247

[8] Yuan, C., Tao, X., Ni, W., Li, N., Jamalipour, A. and Liu, R.P. (2020) Joint Power Allocation and Beamforming for Overlaid Secrecy Transmissions in MIMO-OFDM Channels. *IEEE Transactions on Vehicular Technology*, **69**, 10019-10032. https://doi.org/10.1109/TVT.2020.3004889

[9] Yadav, S. and Gurjar, D.S. (2021) Secrecy Performance of SIMO Underlay Cognitive Radio Networks over α-μ Fading Channels. *IEEE Access*, **9**, 62616-62629. https://doi.org/10.1109/ACCESS.2021.3074507

[10] Kong, L., Kaddoum, G. and da Costa, D.B. (2018) Cascaded α-μ Fading Channels: Reliability and Security Analysis. *IEEE Access*, **6**, 41978-41992. https://doi.org/10.1109/ACCESS.2018.2833423

[11] Kong, L., Kaddoum, G. and Rezki, Z. (2018) Highly Accurate and Asymptotic Analysis on the SOP over SIMO α-μ Fading Channels. *IEEE Communications Letters*, **22**, 2088-2091. https://doi.org/10.1109/LCOMM.2018.2861877